Pergamon

Int. J. Heat Mass Transfer. Vol. 39, No. 6, pp. 1273–1280, 1996

0017-9310/96 $15.00+0.00

0017-9310(95)00201-4

Determination of moisture diffusivity in porous media using moisture concentration profiles

L. PEL and H. BROCKEN

Department of Architecture and Building Technology, Eindhoven University of Technology, P.O. Box 513, 5600 MB Eindhoven, The Netherlands

and

K. KOPINGA

Department of Physics, Eindhoven University of Technology, P.O. Box 513, 5600 MB Eindhoven, The Netherlands

(*Received* 15 *June* 1994 *and in final form* 12 *May* 1995)

Abstract—A procedure is presented to determine the moisture diffusivity for drying from measured moisture concentration profiles. From error analysis it is shown that the applied space grid for scanning and the one-dimensional resolution of the NMR (nuclear magnetic resonance) method used for the measurements had a minor influence on the accuracy of the determination of the moisture diffusivity. The inaccuracy was dominated by experimental noise and inhomogeneities in the porosity of the materials under investigation. A receding drying front method is presented to determine the moisture diffusivity at low moisture contents: here the moisture transport is dominated by vapour transport, which limits the overall drying rate. The method uses the velocity of the receding drying front to approximate the moisture diffusivity.

1. INTRODUCTION

In many areas of research one is interested in the drying of porous media, e.g. chemical engineering, civil engineering and soil science. In these engineering applications one prefers a simple, but correct description, which will simulate the drying of a material correctly. In the spirit of this pragmatic point of view, Philip and de Vries [1] modelled the moisture transport in porous materials during drying by diffusion equations. Various authors, e.g. refs. [2, 3], have tried to derive these equations by means of volume averaging techniques. Although insight into the problem has improved, there is still no correct description of the moisture transport. Especially moisture/vapour interactions and effects of hysteresis on the moisture transport are not yet fully understood. Therefore, the various coefficients have to be determined experimentally. Up to now overall techniques, e.g. drying curves, were often used to determine these coefficients. However, in those cases a relation has to be assumed between the moisture diffusivity coefficient and the actual moisture content, which is not known beforehand. This method will therefore, in general, give an incorrect estimate of the moisture diffusivity [4].

By measuring the moisture concentration profiles during drying, the moisture diffusivity coefficient can be determined directly. In the present study, moisture concentration profiles are determined by nuclear magnetic resonance (NMR). Special attention is given to the various inaccuracies in the determination of the moisture diffusivity. Finally, a new method is presented to determine the moisture diffusivity at low moisture contents, where the drying is dominated by vapour transport.

2. NUCLEAR MAGNETIC RESONANCE

2.1. *General characteristics*

In a nuclear magnetic resonance (NMR) experiment the magnetic moments of the hydrogen nuclei are manipulated by suitably chosen radio frequency fields, resulting in a so-called spin-echo signal. The amplitude of this signal is proportional to the number of nuclei excited by the radio frequency field. NMR is a magnetic resonance technique, where the resonance condition for the nuclei is given by

$$f = \gamma B_0. \tag{1}$$

In this equation f is the frequency of the radio frequency field, γ is the gyromagnetic ratio (for ^{1}H $\gamma = 42.58$ MHz/T), and B_0 is the externally applied static magnetic field. Because of this condition the method can be made sensitive to only hydrogen and therefore to water [5], in contrast to attenuation methods. With NMR, a distinction can also be made between free, physically bound and chemically bound water. When a known magnetic field gradient is applied, the resonance condition will be dependent on the spatial position of the nuclei and the moisture distribution can be measured without moving the sample.

NOMENCLATURE

B	magnetic field strength [T]	x	spatial coordinate [m].
D_θ	isothermal moisture diffusivity [$m^2 s^{-1}$]		
f	resonance frequency [MHz]	Greek symbols	
l	length of the sample [m]	θ	moisture content [$m^3 m^{-3}$]
t	time [s]	γ	gyromagnetic ratio [MHz T^{-1}].

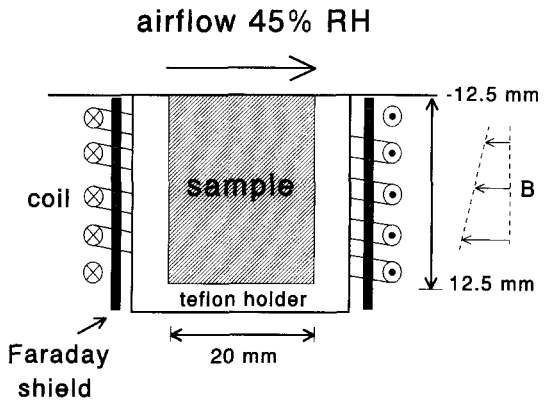

Fig. 1. Experimental probe head for measuring moisture concentration profiles during drying using NMR.

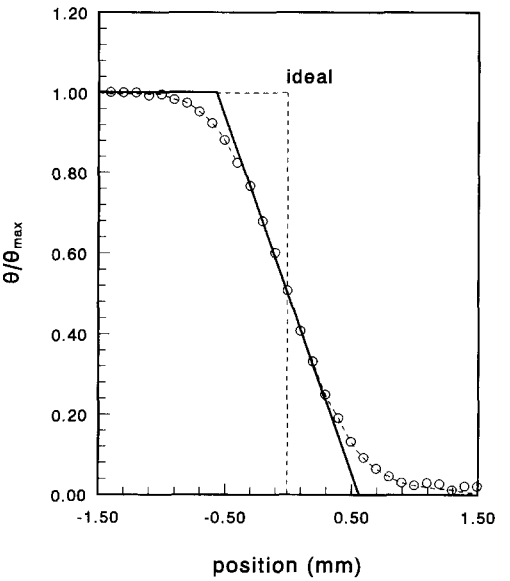

Fig. 2. (○) Measured moisture concentration profile for a sample with a flat bottom. The one-dimensional resolution is 1.0 mm in this case. The dashed line indicates the ideal situation of a one-dimensional resolution of 0 mm.

2.2. *Experimental set-up*

The experiments described in this study were performed using a NMR apparatus especially designed for quantitative moisture measurements in inorganic porous materials [6]. The NMR probe head is given in Fig. 1. The sample, a small cylinder with a length of 25 mm and a diameter of 20 mm, is placed in a teflon holder of which the upper side is open (teflon hardly contains any hydrogen). Air, with a $45 \pm 5\%$ relative humidity (RH) and a temperature of $20 \pm 0.5°C$, is blown over the sample, thus creating a one-dimensional drying experiment.

A coil, which forms part of a tuned LC circuit, is placed around the sample for creating and receiving the radio frequency fields during NMR experiments. The apparatus is designed such that quantitative measurements of the moisture profile can be performed [unlike standard MRI (magnetic resonance imaging), which is generally used in a qualitative way]. Therefore a specially designed Faraday shield is placed between the coil and the sample, to suppress the effects of changes of the dielectric permittivity by variations of the moisture content. The probe head is placed between the poles of an iron-cored electromagnet, which creates a static field of 0.75 T, corresponding to a resonance frequency for ^1H of 32 MHz. With gradient coils, a well defined magnetic field gradient is generated in the vertical direction. To check the absolute accuracy of the measurement and to determine the one-dimensional resolution, the moisture distribution of a completely wetted sample is measured. In this experiment the flat bottom of the sample is located in the middle of the radio frequency coil. The results are given in Fig. 2. The solid line indicates the linearized quantitative response of the NMR apparatus. The one-dimensional resolution is 1.0 mm in this case.

Measuring an entire moisture profile over 25 mm with an inaccuracy of 1% and an equally spaced grid for scanning of 0.15 mm takes typically about 40 min. (This time strongly depends on the magnetic properties of the material under investigation. The spin-lattice relaxation time, T_1, which determines the repetition time ($\approx 4T_1$) of the spin-echo experiment is of the order of 300 ms for the materials considered in this paper.) During the measurements a time stamp is added to each point of such an experimental moisture profile. The moisture concentration profile at a specific time is obtained by interpolating subsequent experimental profiles as a function of time for each position of the grid, using least-squares fits with cubic splines.

3. EXPERIMENTAL RESULTS

Drying experiments were performed with several kinds of building materials: machine moulded fired-clay red brick, sand-lime brick and gypsum, all having an isotropic structure. Each drying experiment was

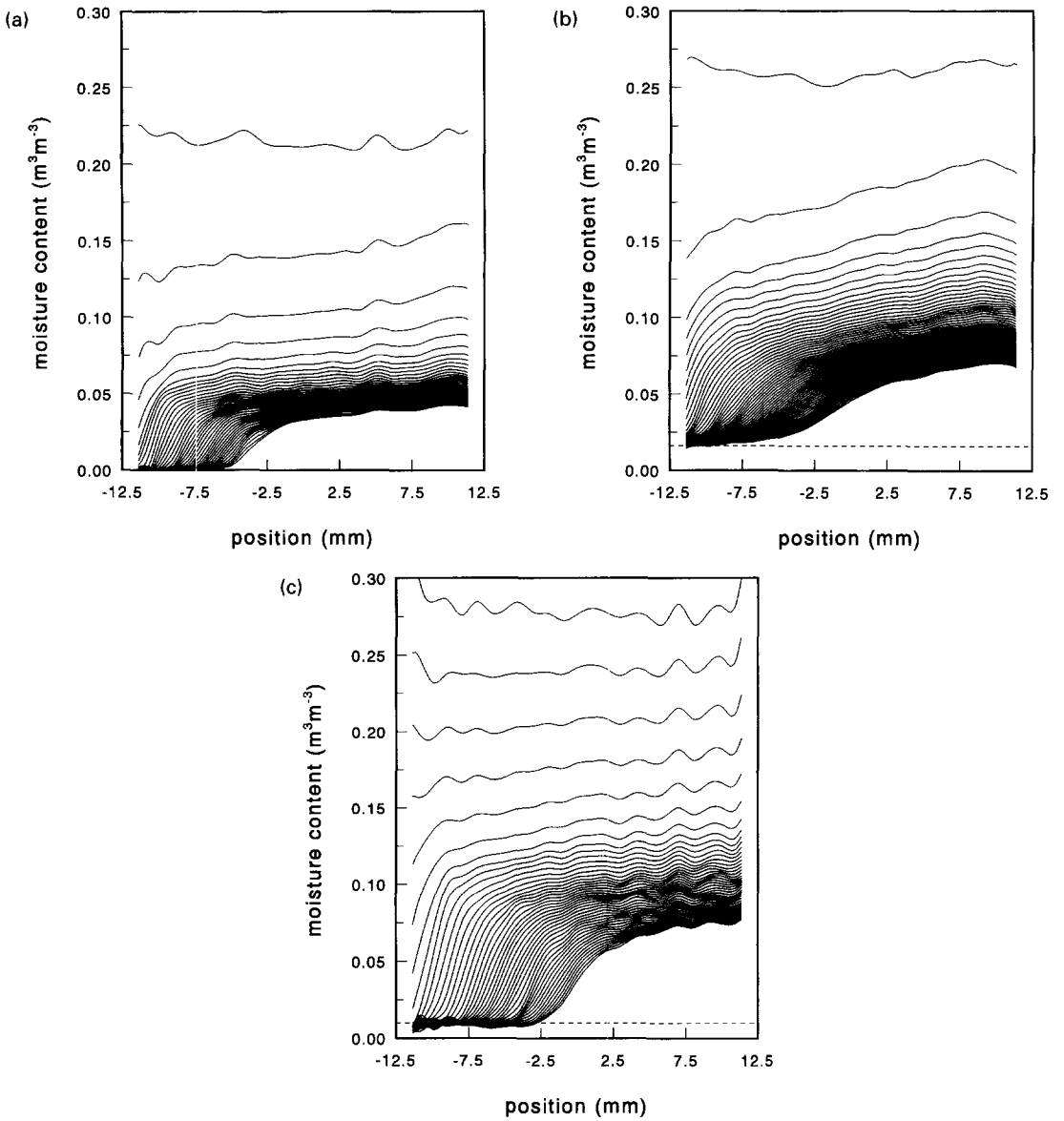

Fig. 3. Moisture concentration profiles measured during drying for fired-clay brick (a), sand-lime brick (b), and gypsum (c). The time between subsequent profiles is 1 h for brick and gypsum, whereas the time between subsequent profiles for sand-lime brick is 2 h. The profiles are given for a period of 42 h for fired-clay brick, 120 h for sand-lime brick and 46 h for gypsum. The horizontal dashed line indicates the residual moisture content observed at 45% relative humidity in these drying experiments.

performed for a period of 40 h or longer. The resulting moisture concentration profiles for the various materials are plotted in Fig. 3. Inspection of the profiles shows variations which are substantially larger than the experimental noise, and reproduce from profile to profile, e.g. for fired-clay brick at a position of 5 mm. These variations reflect the inhomogeneities of the sample.

In all cases a receding drying front is observed after some time. The evolution of the moisture concentration profiles, however, is quite different for the various materials. For both fired-clay brick and gypsum a drying front is observed after approximately 7 h, whereas it takes more than 20 h for a drying front to develop in sand-lime brick. After the drying front has entered the material a residual moisture content is observed for both gypsum and sand-lime brick. The hygroscopic curves for the three materials are given in Fig. 4. These curves were measured by bringing a sample of such a material into contact with air having a certain relative humidity and waiting for equilibrium. For the sorption curve an initially dry sample was used and for the desorption curve an initially wet sample. Hence, each point on such a curve represents an equilibrium situation where no moisture transport occurs. For both gypsum and sand-lime brick a clear hysteresis is present. The residual moisture content that is observed for these materials in our forced dry-

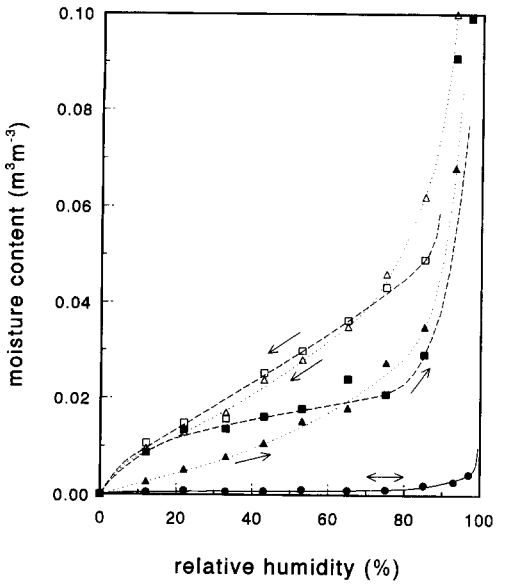

Fig. 4. Hygroscopic curves; the main curves for absorption and desorption measured for the fired-clay brick (●), sand-lime brick (■, □) and gypsum (▲, △).

ing experiment, however, is lower than the corresponding value on the desorption curve. In fact, it is only slightly higher than the corresponding value on the absorption curve for 45% RH. This suggests that during this *forced* drying, a desorption curve ending just above the main absorption curve is followed.

As soon as the drying is started, heat will be extracted and the temperature of the top of the sample will decrease. Because the sample is fitted in a teflon holder, a temperature gradient will develop. In this case the heat flow is a three-dimensional problem. When the receding drying front enters the material, the drying is internally limited by vapour transport and hence the drying rate, and thus the heat extracted from the sample, is strongly decreased. About 2 h later, i.e. about 8 h after the start, the experiment can be regarded as isothermal [7]. This was checked with independent temperature measurements in our experimental set-up [8].

Neglecting the influence of gravity, the moisture transport for the one-dimensional isothermal problem reflecting the experiments can be described by

$$\frac{\partial \theta}{\partial t} = \frac{\partial}{\partial x}\left(D_\theta \frac{\partial \theta}{\partial x}\right). \tag{2}$$

In this equation θ is the actual moisture content, D_θ is the moisture diffusivity, which is a function of the actual moisture content, and x corresponds to the vertical direction in our experiments. To derive the D_θ from the experimental moisture concentration profiles this equation is integrated with respect to x, yielding

$$D_\theta = \frac{\int_1^{x'} \left(\frac{\partial \theta}{\partial t}\right) \mathrm{d}x}{\left(\frac{\partial \theta}{\partial x}\right)_{x'}}. \tag{3}$$

In this equation, use is made of the fact that the partial derivative of θ with respect to x is zero at the vapour tight bottom ($x = l$). The resulting numerically calculated moisture diffusivities are plotted against the corresponding moisture content in Fig. 5. In this figure results are included only for those regions of the material where the effects of inhomogeneities are relatively small and the situation can be regarded as isothermal. For the calculations of the derivative $\partial\theta/\partial x$, local averages of the experimental data were taken to reduce the effect of fluctuations. It is obvious that the data in the figure have a significant scatter which is rather pronounced at both high and low moisture contents. This is directly related to the accuracy by which the derivative of the moisture content with respect to position can be determined. Despite these uncertainties, however, the data clearly reveal a well defined variation of the moisture diffusivity with moisture content.

In the observed behaviour of the moisture diffusivity three regimes can be distinguished, where each can be related to a certain region of the moisture profiles (see Fig. 3). At high moisture contents the moisture transport is dominated by liquid transport: the almost horizontal profiles correspond to a high moisture diffusivity. With decreasing moisture content the large pores will be drained and will therefore, no longer contribute to liquid transport. Subsequently the moisture diffusivity will decrease. Below a so-called critical moisture content, the water in the sample no longer forms a continuous phase. Hence, the moisture has to be transported by vapour and this transport will therefore be governed by the vapour pressure. For small moisture contents the moisture diffusivity starts to increase again. This can be explained by noting that the contribution of the vapour transport to the moisture transport can be related to the slope $\partial\theta/\partial$RH of the hygroscopic curve (see Fig. 4). Starting at 100% relative humidity the slope decreases rapidly; a certain gradient of the moisture content will involve a gradient of the vapour pressure which increases with decreasing moisture content. This will result in an increasing moisture diffusivity at low moisture contents, whose regime corresponds to the almost horizontal profiles at these moisture contents. The minimum moisture diffusivity therefore indicates the transition from moisture transport dominated by liquid transport to moisture transport dominated by vapour transport. This transition from liquid to vapour transport corresponds to the drying front in the moisture profiles.

4. ERROR ANALYSIS

In the determination of the moisture diffusivity from the measured moisture concentration profiles, three main causes of error can be identified: (1) the space grid for scanning; (2) the one-dimensional resolution; and (3) the noise in the moisture content measurement. To investigate the effects of these errors

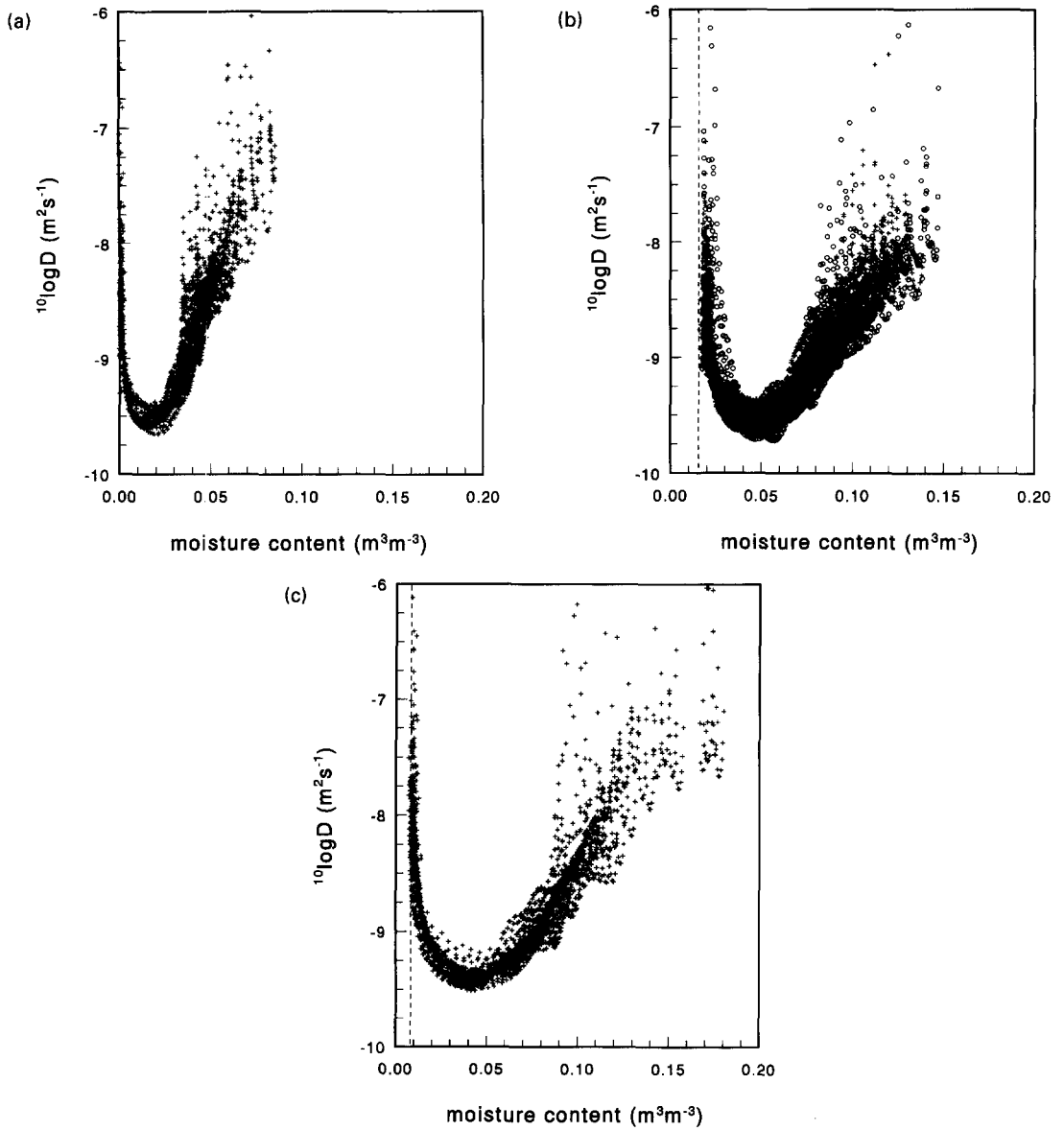

Fig. 5. Moisture diffusivity determined from the measured moisture concentration profiles plotted against the corresponding moisture content for fired-clay brick (a), sand-lime brick (b) and gypsum (c). (+) experimental data, (○) second experiment on a different sample of the same type of material under identical conditions. The vertical dashed line indicates the residual moisture content observed at 45% relative humidity in these drying experiments. Each figure contains over 2000 data points.

and to check the method that was used to calculate the moisture diffusivity from the moisture concentration profiles, computer simulations were done. First, the drying was simulated for an ideal sample using a moisture diffusivity similar to the experimental result obtained for fired-clay brick. These moisture concentration profiles were computed using standard procedures from the NAG-library [9]. As previously shown [7], the space grid for scanning the moisture concentration profile should be as fine as possible to enable a correct determination of the moisture diffusivity. Moisture concentration profiles, with an equally spaced grid of 0.15 mm, were generated from computed ideal profiles. This space grid corresponds to the one used in the NMR measurements. Using these simulated discrete moisture concentration profiles, the moisture diffusivity was recalculated using the method discussed in the previous section. The recalculated moisture diffusivity was found to reproduce the original behaviour within 1% over the full moisture content range. Secondly, the one-dimensional resolution was investigated. If this resolution is too low, the measured profiles will be smoothed and the extrema of the derivative of the moisture content with respect to position will be underestimated. The results of a combined error simulation involving both a 0.15 mm space grid for scanning and a one-dimensional resolution of 1.0 mm (see Fig. 2) are shown in

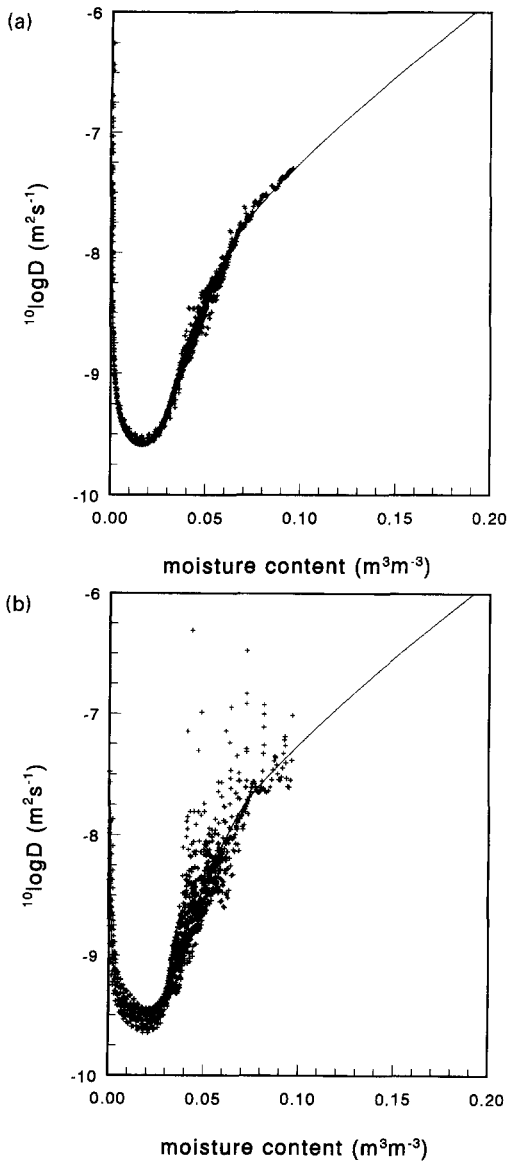

Fig. 6. Moisture diffusivities calculated from simulated moisture concentration profiles plotted against the corresponding moisture content; (a) for an equally spaced grid of 0.15 mm for scanning and a one-dimensional resolution of 1 mm, (b) with 2% random noise added to the simulated moisture concentration profiles. (——) original moisture diffusivity used in the simulations, (+) moisture diffusivity calculated from the simulated concentration profiles.

Fig. 6a. The moisture diffusivity is reproduced well over the full range: only the minimum moisture diffusivity is slightly overestimated.

To check for the influence of noise, 2% random noise was added to the simulated moisture concentration profiles. The results are given in Fig. 6b. The behaviour of the original moisture diffusivity is still rather well reproduced. Moreover, as can be seen from comparison of Figs. 6b and 5a, the characteristics of the experimental results are reproduced correctly. From these simulations it can be concluded that the space grid for scanning and the one-dimensional resolution in our NMR experiments had only a minor influence on the determination of the moisture diffusivity.

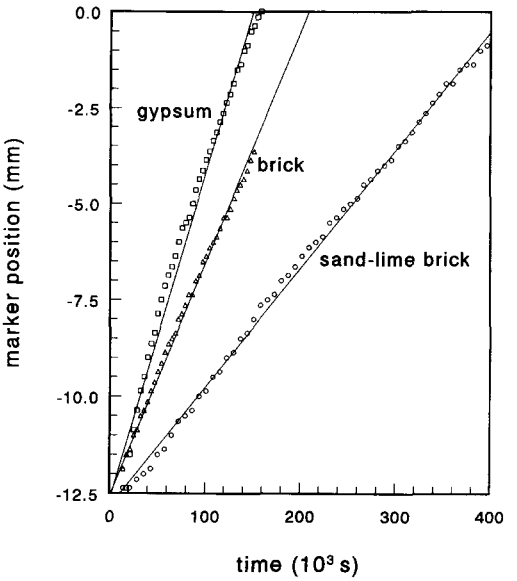

Fig. 7. Position of the marker indicating the receding front plotted against the corresponding time for the various materials.

5. RECEDING DRYING FRONT METHOD

In order to simulate the drying of the materials under investigation, it is very important to determine the moisture diffusivity at low moisture contents correctly. In this regime the moisture transport is dominated by vapour transport, which limits the overall drying rate. However, the experimental and simulated results in Figs. 5 and 6, respectively, reveal that the moisture diffusivity in this range cannot be determined from the measured profiles with sufficient accuracy. Therefore we developed a new method of analysis based on the receding drying front. The velocity at which this front enters the material can be used to approximate the moisture diffusivity at low moisture contents: this diffusivity is approximated such that the receding drying front of the simulation has the same front velocity as the experimentally determined one. To determine the velocity, the position of the front has to be identified as a function of time. The moisture content at the minimum of the moisture diffusivity [roughly corresponding to the maximum of $\partial\theta/\partial x$, cf. equation (3)] was chosen as a marker for the receding front position. In Fig. 7, the position of the front is plotted against the corresponding time for the three materials discussed in this paper. In all cases, the variation of the position with time can be approximated by a linear relation, indicating that the receding front has an almost constant velocity.

The velocity determined in this way is then used to approximate the moisture diffusivity at low moisture contents. To this end, the moisture diffusivity in the

region between the moisture content corresponding to 45% relative humidity and the point where the moisture diffusivity has roughly two times its minimum value is approximated by a straight line (see inset of Fig. 8). In computer simulations of the drying process, the moisture diffusivity at 45% relative humidity is changed until the simulated receding front velocity is identical to the experimentally determined velocity. In addition to the diffusivity determined from drying experiments, the moisture diffusivity found from absorption experiments was used in these simulations (see Appendix) to model the behaviour of the moisture diffusivity at high moisture contents, under the assumption that hysteresis can be neglected. In this respect one should note that the behaviour of the moisture diffusivity at higher moisture contents has only a minor effect on the drying rate, as already indicated above.

In Fig. 8 this procedure is illustrated. The front velocity obtained from the simulations is plotted for the three materials under investigation as a function of the value of the moisture diffusivity at 45% RH. The solid curves represent the results for a sample length of 25 mm, reflecting the experimental situation. The point where such a curve intersects the corresponding experimentally determined front velocity is indicated by a black circle. The dashed curve represents the simulated front velocity for a sample of fired-clay brick with a length of 50 mm. To a fair approximation, it is found that for a twice as long sample the front velocity is twice as low (see Fig. 8). The open circle reflects the intersection of this curve

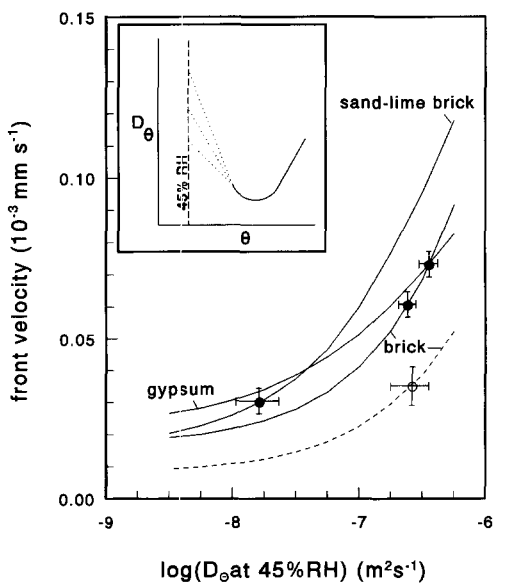

Fig. 8. Calculated front velocity for the various materials as a function of the moisture diffusivity at 45% relative humidity, for samples with a length of 25 mm. The dashed curve is the front velocity for a sample of fired-clay brick with a length of 50 mm. The closed and open circles denote the front velocities determined from the experiments. The inset shows the linear approximation that was used in the computer simulations.

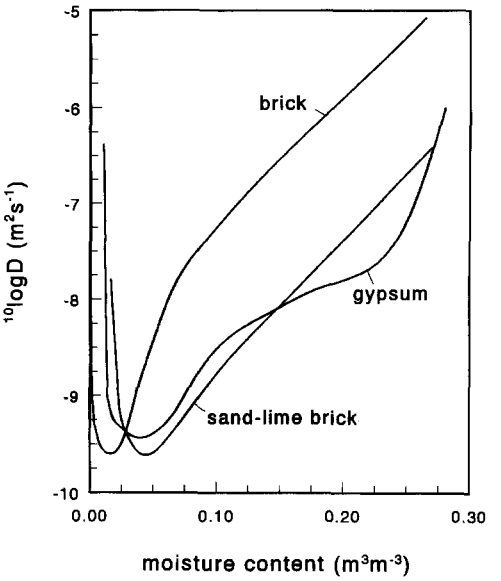

Fig. 9. Moisture diffusivity for drying over the full moisture content range obtained by combining the moisture diffusivities determined from, successively, moisture concentration profiles during absorption, during drying and the receding front method.

with the observed front velocity for such a sample. The figure reveals a good agreement between the moisture diffusivities at 45% RH inferred from the 25 and 50 mm samples of fired-clay brick, suggesting that the receding drying front method is appropriate.

The moisture diffusivity for drying over the full moisture content range for the three materials under investigation can be obtained by combining the moisture diffusivities found from the moisture concentration profiles during drying and during absorption with those obtained from the receding front method. The results of such an approximation are presented in Fig. 9. Finally, in Fig. 10 a computer simulation of the experiment is plotted for fired-clay brick using the behaviour of the moisture diffusivity given in Fig. 9. As expected, the simulated moisture profiles reproduce the experimental profiles given in Fig. 3a very well, except for the first few profiles, indicating that the initial drying rate is underestimated. This may be related to temperature effects, as already indicated in Section 3.

6. CONCLUSIONS

Nuclear magnetic resonance has been shown to be an accurate and reliable method for determining the moisture concentration profiles in porous media. The moisture diffusivity can be determined directly from the measured moisture concentration profiles. The space grid for scanning and the one-dimensional resolution had only a minor influence. The error in the calculation of the moisture diffusivity was dominated by experimental noise and inhomogeneities in the porosity of the material.

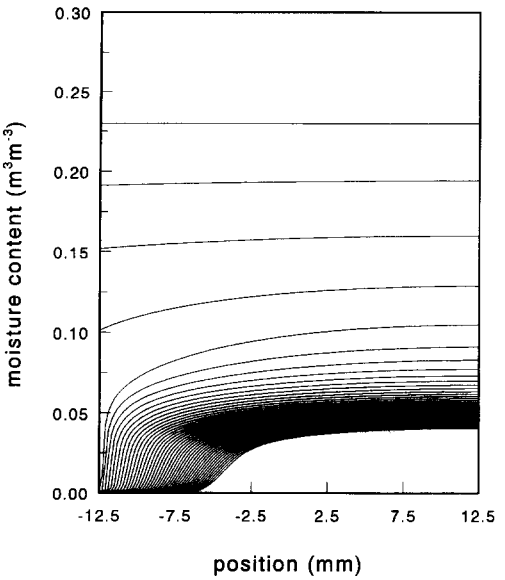

Fig. 10. A computer simulation of the drying of fired-clay brick using the moisture diffusivity plotted in Fig. 9. The time between subsequent profiles is 1 h and the profiles are given for a total period of 48 h.

The velocity of the receding drying front was found to be constant and to a fair approximation inversely proportional to the length of the sample (cf. Fig. 8). Using the experimentally observed velocity of the receding front, the moisture diffusivity can be approximated in such a way that it will correctly model the moisture concentration profiles during drying.

Acknowledgements—The authors wish to thank J. Noyen, H. Otten, H. Smulders and A. W. B. Theuws for their indispensable help in building the equipment and performing the experiments. We also like to thank W. J. M. de Jonge for the support he has given to the NMR experiments. This project was financially supported by the Royal Association of Dutch Brick Manufacturers (KNB).

REFERENCES

1. J. R. Philip and D. A. de Vries, Moisture movement in porous materials under temperature gradients, *Trans. Am. Geophys. Un.* **38,** 222–232 (1957).
2. J. Bear and Y. Bachmat, *Introduction to Modelling of Transport Phenomena in Porous Media*, Vol. 4. Kluwer, Dordrecht (1990).
3. S. Withaker, Simultaneous heat, mass and momentum transfer in porous media. A theory of drying porous media, *Adv. Heat Transfer* **13,** 119–200 (1977).
4. A. A. J. Ketelaars, Drying deformable media, Ph.D. thesis, Eindhoven University of Technology, The Netherlands (1992).
5. R. L. Dixon and K. E. Ekstrand, The physics of proton NMR, *Med. Phys.* **9,** 807–818 (1982).
6. K. Kopinga and L. Pel, One dimensional scanning of moisture in porous materials with NMR, *Rev. Sci. Instrum.* **65,** 3673–3681 (1994).
7. L. Pel, A. A. J. Ketelaars, O. C. G. Adan and A. A. van Well, Determination of moisture diffusivity in porous media using scanning neutron radiography, *Int. J. Heat Mass Transfer* **36,** 1261–1267 (1993).
8. L. Pel, Moisture transport in porous building materials, Ph.D. thesis, Eindhoven University of Technology, The Netherlands (1995).
9. The NAG Numerical Fortran Library, Mark 15. NAG, Oxford, (1991).

APPENDIX
MOISTURE DIFFUSIVITY FOR ABSORPTION

To determine the moisture diffusivity for absorption, the moisture concentration profiles during absorption of water by samples of the same type of material were measured using NMR. If the well known Boltzmann transformation, $\lambda = xt^{-1/2}$, is applied, equation (2) reduces to the ordinary differential equation

$$2\frac{\mathrm{d}}{\mathrm{d}\lambda}\left(D_\theta\frac{\mathrm{d}\theta}{\mathrm{d}\lambda}\right)+\lambda\frac{\mathrm{d}\theta}{\mathrm{d}\lambda}=0. \tag{A1}$$

Using the boundary conditions for absorption: $\theta = \theta_{atm}$ at $\lambda = 0$ and $\theta = \theta_0$ as $\lambda \to \infty$, this equation has only one solution, so all profiles are related by a simple $t^{1/2}$ scaling. The moisture profiles after the Boltzmann transformation for the three materials under investigation are given in Fig. A1. For all materials the Boltzmann transformation is satisfied, as shown by the distinct curves on which the individual moisture profiles for each material collapse. Using the transformed sets of data, the moisture diffusivity for absorption can be determined by integrating equation (A1), yielding

$$D_\theta = -\frac{1}{2}\frac{1}{\left(\dfrac{\mathrm{d}\theta}{\mathrm{d}\lambda}\right)_\theta}\int_{\theta_0}^{\theta}\lambda\,\mathrm{d}\theta'. \tag{A2}$$

The resulting moisture diffusivities are included in Fig. 9. These results were also used to perform computer simulations of the transformed moisture concentration profiles, which are represented by solid curves in Fig. A1.

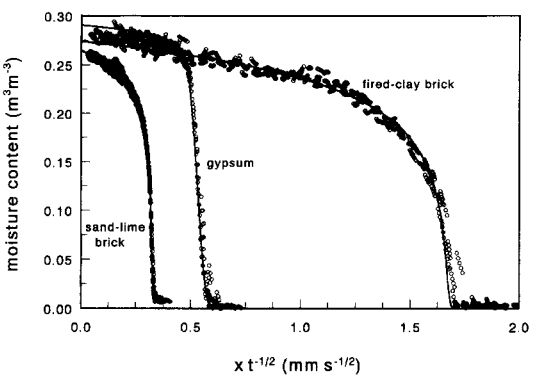

Fig. A1. Measured moisture concentration profiles for absorption after Boltzmann transformation. (—) Simulated moisture concentration profiles using the moisture diffusivity for absorption calculated from the corresponding data.